Elastic buckling finite strip analysis of the AISC sections database and proposed local plate buckling coefficients

Authors:

Mina Seif, Johns Hopkins University, MD, mina.seif@jhu.edu
Benjamin Schafer, Johns Hopkins University, MD, schafer@jhu.edu

ABSTRACT

The objective of this paper is to provide analytical expressions for the elastic cross-section local buckling stress, including element interaction, of hot-rolled steel structural shapes. The cross-section local buckling stress is determined by finite strip analysis. Local stability of each cross-section is considered in axial compression, as well as positive and negative bending about the major and minor axis. All sections in the AISC shapes database are considered, with the exception of pipe sections. The local buckling stresses are converted into plate buckling coefficients (*k*'s) and simplified expressions provided for all observed *k*'s. The plate buckling coefficients (*k*'s) from the finite strip analysis are also compared to the values inherently assumed in the AISC Specification. Significant differences between assumed (AISC) and calculated *k* values are observed.

INTRODUCTION

In hot-rolled steel structural design local bucking of the cross-section is avoided by adherence to the compactness limits provided in Table B4.1 of the AISC Specification [AISC 2005]. In the rare case in current design where local buckling must be considered, the compactness limits of Table B4.1 are still employed in the strength prediction expressions. Thus, the assumptions regarding local buckling, inherent in Table B4.1, are essential to the AISC Specification. One key assumption is that any interaction that may exist between the flange and the web of a cross-section is fixed for a given cross-section type.

Further refinement of AISC's basic approach to local buckling may be warranted. For one, the dominant philosophy in hot-rolled steel design is to avoid local buckling, but this may waste material and ignores the beneficial post-buckling reserve that exists in these modes (in fact the AISC Specification essentially ignores post-bucking in flanges). Second, detailed interactions between the elements of the cross-section in local buckling may now be treated with relative computational ease, as demonstrated in this paper. Third, local buckling is the desired ultimate limit state in extreme loading cases and the accuracy of local buckling prediction needs improvement as prediction of performance in extreme loading becomes more a part of typical design. Finally, adoption of high and ultrahigh yield strength steels increases the propensity for local buckling in all structural steel shapes. Given these reasons, this paper investigates one possible improvement to local buckling prediction, the inclusion of element interaction in prediction of the local buckling stress.

The interaction of elements of a cross-section (e.g., the web and the flange) in local buckling has been examined, even in structural steel shapes, for some time. For example Bijlaard and Fisher [1953] present relationships for flange local plate buckling coefficients in terms of cross-section dimensions, half wavelength of the buckled shape, and flange flexural rigidity. More complete nomgraphs may also be found in the literature [e.g., Bulson 1970] including those using the finite strip method [Hancock 1978]. The objective here is to provide a set of simple design expressions for local buckling which include element interaction in a manner similar to these earlier nomogrpahs, but (a) in a form more amenable to design and (b) covering all structural steel shapes under all anticipated loading cases.

AISC LOCAL BUCKLING CRITERIA:

In this section the local buckling width-to-thickness limits of the AISC Specification are examined, and a method provided for determining the assumed local plate buckling coefficients (*k*'s) inherent in the AISC Specification. Currently, the AISC Specification defines, in Table B4.1, the local buckling criteria in terms of width-to-thickness ratios, i.e., for an element of width *b*, and thickness, *t*:

$$\lambda = \frac{b}{t} \tag{1}$$

The elastic critical local buckling stress of this element is

$$f_{cr} = k\frac{\pi^2 E}{12\left(1-\nu^2\right)}\left(\frac{t}{b}\right)^2 = k\frac{\pi^2 E}{12\left(1-\nu^2\right)}\left(\frac{1}{\lambda}\right)^2 \tag{2}$$

where E is Young's modulus, ν is Poisson's ratio, and k is the local plate buckling coefficient which accounts for the boundary conditions and loading.

Plate slenderness, as originally utilized [e.g. von Karman et al., 1932], is expressed as

$$\alpha = \sqrt{f_y / f_{cr}} \tag{3}$$

where f_y is the yield stress. Note the usual notation for plate slenderness is λ, but AISC uses this symbol for b/t, so the symbol α has been adopted here for plate slenderness. The AISC compactness limits, λ_r (associated with α_r) define the non-slender/slender element limits for columns or the non-compact/slender element limit for beams as:

$$\lambda_r = \left(\frac{b}{t}\right)_r = \beta_r\sqrt{E / f_y} \tag{4}$$

where β_r is given for different element types and loading conditions in AISC Table B4.1. The inter-relationship between the plate buckling coefficient, k, plate slenderness limit, α_r, and width-to-thickness ratio coefficient β_r may be found by substituting f_{cr} from (2) into (3) and solving for the $(b/t)_r$ limit of (4):

$$\sqrt{k\frac{\pi^2}{12\left(1-\nu^2\right)}\alpha_r^{\,2}}\sqrt{E / f_y} = \left(\frac{b}{t}\right)_r \tag{5}$$

Using (4) and solving for k results in:

$$k = \frac{\beta_r^{\,2}}{\alpha_r^{\,2}} \frac{12\left(1-\nu^2\right)}{\pi^2} \tag{6}$$

Implying that, if the plate slenderness limit α_r is known, and given β_r is provided (from AISC Table B4.1) then the k value assumed by the AISC Specification may be back-calculated.

The plate slenderness limits α_r are generally determined from testing. For compression AISC employs an α_r=0.7 (which itself implies f_{cr}=2f_y) [e.g., see Salmon et al. 2009]. This agrees well with Winter's equation, employed extensively in cold-formed steel design [AISI 2007], where α_r=0.673. The k value assumed in AISC may now be found for any section, for example, consider the case of compression in webs of doubly symmetric I-shaped sections, β_r is 1.49 (from Table B4.1), which will yield a k value of 5.0 when using α_r of 0.7; which is about one-third of the way between simply supported (k = 4.0) and fixed (k = 6.97) boundary conditions.

For flexural members, much less is provided in the literature about the assumed plate slenderness limit, α_r. The best discussion the authors have been able to find is provided in relation to plate girders where the criteria α_r=1.0 is clearly employed (which implies f_{cr}=f_y) [Salmon et al. 2009]. For doubly symmetric I-shaped sections in flexure Table B4.1 provides a β_r of 5.7, assuming α_r=1.0 results in a k of 36, which is about 80% between the range of simply supported (k = 23.9) and fixed (k = 39.6) boundary conditions, and this k is consistent with the discussions in White [2008] and Salmon et al. [2009]. It is worth noting that cold-formed steel design [AISI 2007] uses α_r=0.673 for elements in flexure as well as in compression.

LOCAL BUCKLING FINITE STRIP ANALYSIS

Finite strip analysis was performed on all sections in the AISC shape database (v3) from the Manual of Steel Construction (excluding pipe sections) [AISC 2005]. The analysis was completed using CUFSM version 3.12 [Schafer and Ádány 2006]. Sections were simplified to their centerline geometry (the increased width in the k-zone was thus ignored) and analyzed under different loading conditions: axial compression, positive and negative major-axis bending, and positive and negative minor-axis bending.

The cross-section elastic local buckling stress, $f_{cr\ell}$, is found from the finite strip analysis. The local buckling stress is converted into local plate buckling coefficients (k's) for comparison to existing design provisions and for the development of the new approximate design expressions as follows. The plate buckling solution for the flange is:

$$f_{crb} = k_f \frac{\pi^2 E}{12\left(1-\nu^2\right)}\left(\frac{t_f}{b}\right)^2 \tag{7}$$

where k_f is the flange (horizontal element) local plate buckling coefficient (noted as k_b for angles and box sections), b is the unsupported flange width (i.e., ½ of b_f for a W-section, b_f is the total flange width), t_f is the flange thickness, E is the Modulus of elasticity, and ν is Poisson's ratio. Setting f_{crb} = $f_{cr\ell}$ (from the finite strip analysis) and solving for k_f:

$$k_f = f_{cr\ell} \frac{12\left(1-\nu^2\right)}{\pi^2 E}\left(\frac{b}{t_f}\right)^2 \tag{8}$$

Similarly, the web buckling coefficient, k_w, can be found, where:

$$f_{crh} = k_w \frac{\pi^2 E}{12\left(1-\nu^2\right)}\left(\frac{t_w}{h}\right)^2 \tag{9}$$

And setting $f_{crh} = f_{cr\ell}$, we can solve for k_w as:

$$k_w = f_{cr\ell} \frac{12\left(1-\nu^2\right)}{\pi^2 E}\left(\frac{h}{t_w}\right)^2 \tag{10}$$

where k_w is the web (vertical element) local plate buckling coefficient (noted as k_d for angles and box sections), h is the clear distance between flanges less the fillet [see AISC 2005], and t_w is the web thickness. Using the full cross-section elastic local buckling stress, $f_{cr\ell}$, the plate buckling coefficients resulting from (8) and (10) will thus include web-flange interaction.

RESULTS

Consider the AISC W-sections as an example; the flange plate buckling coefficient, k_f, including web-flange interaction can be calculated from each finite strip analysis from (8). For the AISC W-sections in pure compression, the resulting k_f's are provided in Figures 1(a) and (b). Figure 1(a) highlights that the flange plate buckling coefficient is not independent of the web slenderness h/t_w, i.e., web-flange interaction is real and unavoidable. Figure 1(b) shows that if both web and flange slenderness are considered, relatively simple functional relationships may exist for predicting when local buckling occurs. The web plate buckling coefficients are provided for the W-sections in pure compression in Figures 1(c) and 1(d). The web plate buckling coefficient is dependent on the flange slenderness, but again a simple combination of slenderness may adequately describe the plate buckling coefficient, as shown in Figure 1(d). The same observations are true for the different loading cases for all types of sections.

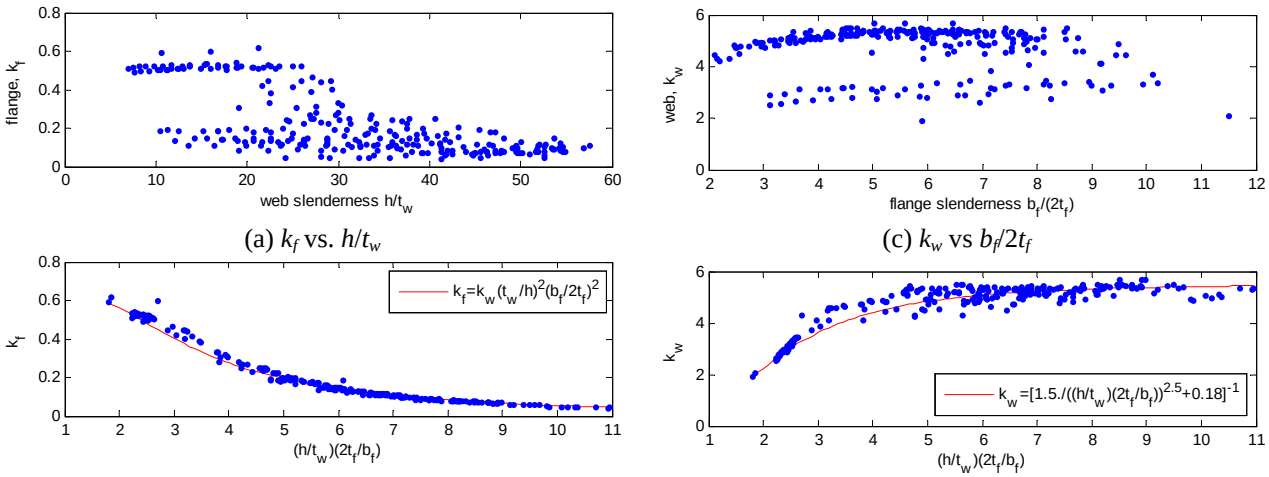

(a) k_f vs. h/t_w

(c) k_w vs $b_f/2t_f$

(b) k_f vs. $h/t_w \cdot 2t_f/b_f$

(d) k_w vs. $h/t_w \cdot 2t_f/b_f$

FIGURE 1 - FLANGE AND WEB LOCAL BUCKLING COEFFICIENTS FOR W-SECTIONS UNDER AXIAL LOADING.

Comparison to AISC Specification limits

AISC Table B4.1 provides the limiting width-to-thickness ratios for local buckling. Using the methodology discussed within this paper, in Table 1 an expanded version of Table B4.1 has been constructed that provides the underlying assumptions of Table B4.1 and compares them to a full cross-section elastic buckling analysis. Table 1 includes both the λ_p and λ_r slenderness limits. As discussed previously these slenderness limits are determined from an assumed plate slenderness limit (α of (3)). The α or $(f_y/f_{cr})^{0.5}$ values associated with each λ limit are also provided in Table 1. Finally, Table 1 provides the *k* value assumed by the AISC Specification, the mean *k* value from the finite strip analysis for the related section, and a histogram of all observed *k* values for local buckling of the related section from the AISC shapes database.

Comparison of the AISC assumed *k* values with those from the finite strip analysis indicates (a) the *k* values fall in a wide range and use of a single *k* value is bound to be quite approximate, and (b) in some cases AISC falls near the mean *k* value predicted from finite strip analysis in other cases it may be significantly higher or lower than the mean. For example, for tees the AISC values are quite near the mean *k* values, while for W-sections the cases of the flange in flexure and the web in compression are near the mean *k* values, while the cases of the web in flexure and the flange in compression are significantly higher (unconservative) compared with the mean finite strip *k* values. To judge the actual impact of the selected *k* values they must be taken in the context of the AISC Specification, for instance, a high *k* value for an unstiffened element may have little impact given that post-buckling of slender unstiffened elements is essentially ignored in the AISC Specification. Nonetheless, the lack of a consistent rational basis for the assumed *k* values employed in the AISC Specification would seem to be an impediment to advancing prediction of local buckling phenomenon.

Development of approximate local buckling coefficients expressions

As shown in Figure 1 simple functional relations exist such that the local plate buckling coefficients can be expressed as a function of section geometry. Further, note that using the same cross-section elastic local buckling stress, $f_{cr\ell}$, instead of the individual f_{crb} and f_{crh}, implies that (7) and (9) must be equal, thus the flange and web local buckling coefficients are related by:

$$k_f = k_w\left(\frac{t_w}{h}\right)^2\left(\frac{b}{t_f}\right)^2 \quad \text{or} \quad k_w = k_f\left(\frac{t_f}{b}\right)^2\left(\frac{h}{t_w}\right)^2 \tag{11}$$

Due to (11) only one local plate buckling coefficient needs to be determined for a cross-section. Therefore, for each loading case, either k_f or k_w was selected and a series of simple empirical equations were developed to provide an approximate means of predicting the local plate buckling coefficients. Table 2 provides the suggested plate buckling coefficients expressions for different section types under the different loading cases. Table 2 represents a potential beginning for the evolution of Table B4.1 in the AISC Specification for analyzing local stability.

Note that the *k* expressions were developed to best match the results obtained from the finite strip analysis of the sections in the AISC shape database. Applying these expressions for sections with dimensions falling outside the range of the current database will need further assessment for accuracy. Finite strip analysis may still be used for sections or loading not covered herein.

				λ_p		λ_r		***k* values**			**Example**
				Limit	$\sqrt{\frac{f_y}{f_{cr}}}$	**Limit**	$\sqrt{\frac{f_y}{f_{cr}}}$	**AISC***	**Mean**	**Histogram**	
Unstiffened Elements	1	Flexure in flanges of rolled I-shaped sections and channels	b/t	$0.38\sqrt{\frac{E}{F_y}}$	0.46	$1.0\sqrt{\frac{E}{F_y}}$	1.0	1.11	1.18	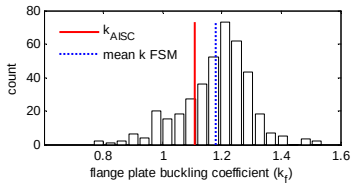	
	2	Flexure in flanges of doubly and singly symmetric I-shaped built up sections	b/t	$0.38\sqrt{\frac{E}{F_y}}$	0.46	$0.95\sqrt{\frac{k_c E}{F_L}}$	1.19	k_c	NA	NA	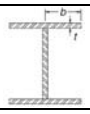
	3	Uniform compression in flanges of rolled I-shaped sections, plates projecting from rolled I-shaped sections; outstanding legs of pairs of angles in continuous contact and flanges of channels	b/t	NA	-	$0.56\sqrt{\frac{E}{F_y}}$	0.7	*0.70*	0.23	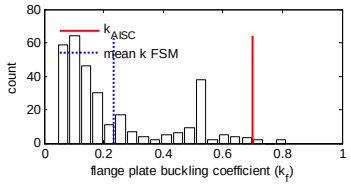	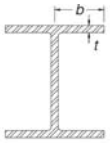
	4	Uniform compression in flanges of built-up I-shaped sections and plates or angle legs projecting from built-up I-shaped sections	b/t	NA	-	$0.64\sqrt{\frac{k_c E}{F_L}}$	0.673	k_c	NA	NA	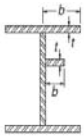
	5	Uniform compression in legs of single angles, legs of double angles with separators, and all other unstiffened elements	b/t	NA	-	$0.45\sqrt{\frac{E}{F_y}}$	0.726	0.425	0.45	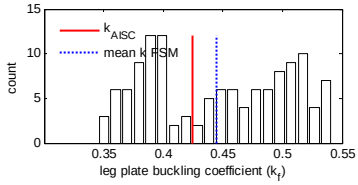	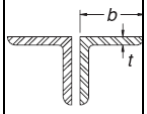
	6	Flexure in legs of single angles	b/t	$0.54\sqrt{\frac{E}{F_y}}$	0.46	$0.91\sqrt{\frac{E}{F_y}}$	1.0	0.92	2.16	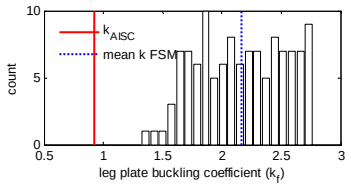	
	7	Flexure in flanges of tees	b/t	$0.38\sqrt{\frac{E}{F_y}}$	0.46	$1.0\sqrt{\frac{E}{F_y}}$	1.0	1.11	1.17	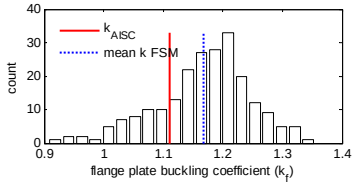	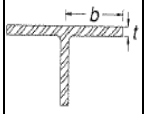
	8	Uniform compression in stems of tees	d/t	NA	-	$0.75\sqrt{\frac{E}{F_y}}$	0.7	1.277	1.25	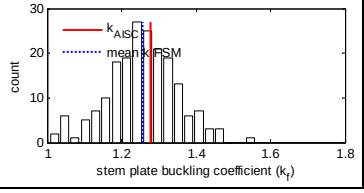	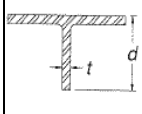

Stiffened Elements	9	Flexure in webs of doubly symmetric I-shaped sections and channels	h/t_w	$3.76\sqrt{\frac{E}{F_y}}$	0.58	$5.70\sqrt{\frac{E}{F_y}}$	1.0	36	15.0	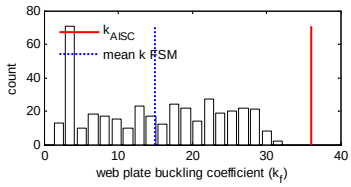	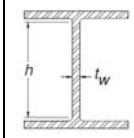
	10	Uniform compression in webs of doubly symmetric I-shaped sections	h/t_w	NA	-	$1.49\sqrt{\frac{E}{F_y}}$	0.7	5.0	4.54	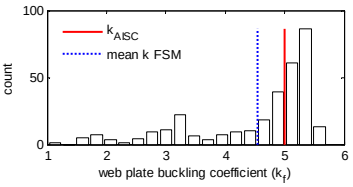	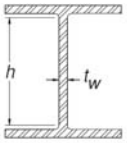
	11	Flexure in webs of singly-symmetric I-shaped sections	h_c/t	$\frac{\frac{h_c}{h_p}\sqrt{E/F_y}}{\left(0.54\frac{M_p}{M_y}-0.09\right)} \le \lambda_r$	0.58	$5.70\sqrt{\frac{E}{F_y}}$	1.0	36	NA	NA	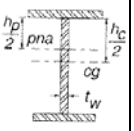
	12	Uniform compression in flanges of rectangular box and hollow structural sections of uniform thickness subject to bending or compression; flange cover plates and diaphragm plates between lines of fasteners or welds	b/t	$1.12\sqrt{\frac{E}{F_y}}$	0.58	$1.40\sqrt{\frac{E}{F_y}}$	0.7	4.43	4.85	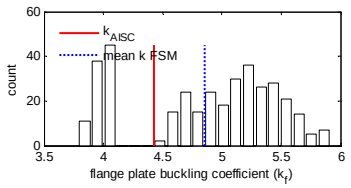	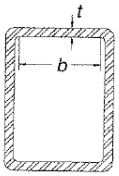
	13	Flexure in webs of rectangular HSS	h/t	$2.42\sqrt{\frac{E}{F_y}}$	0.58	$5.7\sqrt{\frac{E}{F_y}}$	1.0	36	15.3	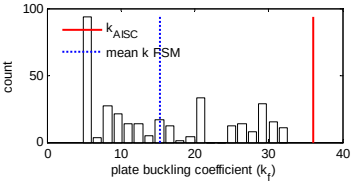	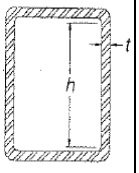
	14	Uniform compression in all other stiffened elements	b/t	NA	-	$1.49\sqrt{\frac{E}{F_y}}$	0.683	5.0	NA	NA	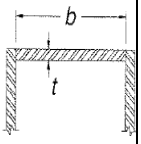
	15	Circular hollow sections In uniform compression In Flexure	D/t D/t	NA $0.07\frac{E}{F_y}$	- 0.58	$0.11\frac{E}{F_y}$ $0.31\frac{E}{F_y}$	NA NA	NA NA	NA NA	NA	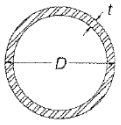

*The theoretical limits provided here are the limits for an isolated plate which has simple supports at the loaded edges and varying support along the longitudinal edges, see [Galambos 1998] or [Salmon and Johnson [1996].

TABLE 1 LOCAL BUCKLING OF AISC SHAPES COMPARED WITH AISC WIDTH-TO-THICKNESS LIMITS AND UNDERLYING PLATE BUCKLING COEFFICIENTS AND SLENDERNESS LIMITS

	Example	***Loading Type***	***Suggested k expression***	f_{cr}	$\sqrt{k_i / k_j}$ *
W, M, S, HP	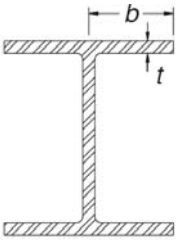	Axial Compression	$\frac{1}{k_w} = 1.5 / \left(\left(\frac{h}{t_w} \right) \left(\frac{2t_f}{b_f} \right) \right)^{2.5} + 0.18$	$f_{crh} = k_w \frac{\pi^2 E}{12(1-\nu^2)} \left(\frac{t_w}{h} \right)^2$	$\left(\frac{t_w}{h} \right) \left(\frac{b_f}{2t_f} \right)$
		Major axis bending (+ve/-ve)	$\frac{1}{k_w} = 1.5 / \left(\left(\frac{h}{t_w} \right) \left(\frac{2t_f}{b_f} \right) \right)^{2} + 0.015$	$f_{crh} = k_w \frac{\pi^2 E}{12(1-\nu^2)} \left(\frac{t_w}{h} \right)^2$	$\left(\frac{t_w}{h} \right) \left(\frac{b_f}{2t_f} \right)$
		Minor axis bending (+ve/-ve)	$\frac{1}{k_w} = 1.5 / \left(\left(\frac{h}{t_w} \right) \left(\frac{2t_f}{b_f} \right) \right)^{2.5} + 0.008$	$f_{crh} = k_w \frac{\pi^2 E}{12(1-\nu^2)} \left(\frac{t_w}{h} \right)^2$	$\left(\frac{t_w}{h} \right) \left(\frac{b_f}{2t_f} \right)$
C, MC	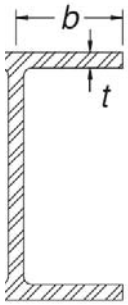	Axial Compression	$k_f = 2.0 / \left(\left(\frac{d}{t_w} \right) \left(\frac{t_f}{b_f} \right) \right)^{1.2} - 0.05$	$f_{crb} = k_f \frac{\pi^2 E}{12(1-\nu^2)} \left(\frac{t_f}{b_f} \right)^2$	$\left(\frac{t_f}{b_f} \right) \left(\frac{d}{t_w} \right)$
		Major axis bending (+ve/-ve)	$\frac{1}{k_w} = 1.1 / \left(\left(\frac{d}{t_w} \right) \left(\frac{t_f}{b_f} \right) \right)^{2} + 0.02$	$f_{crh} = k_w \frac{\pi^2 E}{12(1-\nu^2)} \left(\frac{t_w}{d} \right)^2$	$\left(\frac{t_w}{d} \right) \left(\frac{b_f}{t_f} \right)$
		Minor axis bending (+ve)	$\frac{1}{k_w} = 0.8 / \left(\left(\frac{d}{t_w} \right) \left(\frac{t_f}{b_f} \right) \right)^{2}$	$f_{crh} = k_w \frac{\pi^2 E}{12(1-\nu^2)} \left(\frac{t_w}{d} \right)^2$	$\left(\frac{t_w}{d} \right) \left(\frac{b_f}{t_f} \right)$
		Minor axis bending (-ve)	$k_f = 6.0 / \left(\left(\frac{d}{t_w} \right) \left(\frac{t_f}{b_f} \right) \right)^{2.4}$	$f_{crb} = k_f \frac{\pi^2 E}{12(1-\nu^2)} \left(\frac{t_f}{b_f} \right)^2$	$\left(\frac{t_f}{b_f} \right) \left(\frac{d}{t_w} \right)$
L	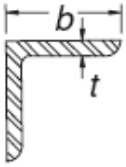	Axial Compression	$k_d = 0.38 / \left(\frac{d}{b} \right)^{1.3}$	$f_{crh} = k_d \frac{\pi^2 E}{12(1-\nu^2)} \left(\frac{t}{d} \right)^2$	$\left(\frac{b}{d} \right)$
		Major axis bending (+ve)	$k_d = 1.2 / \left(\frac{d}{b} \right)^{2}$	$f_{crh} = k_d \frac{\pi^2 E}{12(1-\nu^2)} \left(\frac{t}{d} \right)^2$	$\left(\frac{b}{d} \right)$
		Major axis bending (-ve)	$\frac{1}{k_b} = 1.2 / \left(\frac{d}{b} \right)^{1.3}$	$f_{crb} = k_b \frac{\pi^2 E}{12(1-\nu^2)} \left(\frac{t}{b} \right)^2$	$\left(\frac{d}{b} \right)$
		Minor axis bending (+ve)	$\frac{1}{k_b} = 0.9 / \left(\frac{d}{b} \right)^{2}$	$f_{crb} = k_b \frac{\pi^2 E}{12(1-\nu^2)} \left(\frac{t}{b} \right)^2$	$\left(\frac{d}{b} \right)$
		Minor axis bending (-ve)	$\frac{1}{k_b} = 1.2 / \left(\frac{d}{b} \right)^{0.8}$	$f_{crb} = k_b \frac{\pi^2 E}{12(1-\nu^2)} \left(\frac{t}{b} \right)^2$	$\left(\frac{d}{b} \right)$

WT, MT, ST	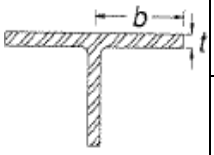	Axial Compression	$k_f = 1.3 / \left(\left(\frac{h}{t_w} \right) \left(\frac{2t_f}{b_f} \right) \right)^2$	$f_{crb} = k_f \frac{\pi^2 E}{12(1-\nu^2)} \left(\frac{2t_f}{b_f} \right)^2$	$\left(\frac{2t_f}{b_f} \right) \left(\frac{h}{t_w} \right)$
		Major axis bending (+ve)	$k_f = 1.8 / \left(\left(\frac{h}{t_w} \right) \left(\frac{2t_f}{b_f} \right) \right)^2$	$f_{crb} = k_f \frac{\pi^2 E}{12(1-\nu^2)} \left(\frac{2t_f}{b_f} \right)^2$	$\left(\frac{2t_f}{b_f} \right) \left(\frac{h}{t_w} \right)$
		Major axis bending (-ve)	$\frac{1}{k_w} = 0.6 / \left(\left(\frac{h}{t_w} \right) \left(\frac{2t_f}{b_f} \right) \right)^{1.5} + 0.01$	$f_{crh} = k_w \frac{\pi^2 E}{12(1-\nu^2)} \left(\frac{t_w}{h} \right)^2$	$\left(\frac{t_w}{h} \right) \left(\frac{b_f}{2t_f} \right)$
		Minor axis bending (+ve/-ve)	$\frac{1}{k_w} = 0.8 / \left(\left(\frac{h}{t_w} \right) \left(\frac{2t_f}{b_f} \right) \right)^2$	$f_{crh} = k_w \frac{\pi^2 E}{12(1-\nu^2)} \left(\frac{t_w}{h} \right)^2$	$\left(\frac{t_w}{h} \right) \left(\frac{b_f}{2t_f} \right)$
HSS	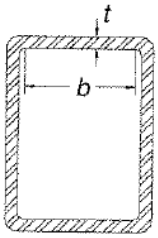	Axial Compression	$k_b = 4.0 / \left(\frac{h}{b} \right)^{1.7}$	$f_{crb} = k_b \frac{\pi^2 E}{12(1-\nu^2)} \left(\frac{t}{b} \right)^2$	$\left(\frac{h}{b} \right)$
		Major axis bending (+ve/-ve)	$\frac{1}{k_h} = 0.19 / \left(\frac{h}{b} \right)^3 + 0.03$	$f_{crh} = k_h \frac{\pi^2 E}{12(1-\nu^2)} \left(\frac{t}{h} \right)^2$	$\left(\frac{b}{h} \right)$
		Minor axis bending (+ve/-ve)	$k_b = 5.5 / \left(\frac{h}{b} \right)^2$	$f_{crb} = k_b \frac{\pi^2 E}{12(1-\nu^2)} \left(\frac{t}{b} \right)^2$	$\left(\frac{h}{b} \right)$

* The relation between the web and flange plate buckling coefficients, where the k_i is the web or flange coefficient calculated from the expression provided, and k_j is the other one as shown in (11).

TABLE 2 - PLATE BUCKLING EXPRESSIONS FOR DIFFERENT SECTIONS UNDER DIFFERENT LOADING CONDITIONS.

CONCLUSIONS

Consideration of local buckling is an important part of the design of structural steel shapes. Increased consideration of ultimate limit states in extreme loading, and the advent of high and ultra-high strength steels make consideration of local buckling of even greater importance today. The primary means for consideration of local buckling in the AISC Specification is the use of width-to-thickness limits for each element of a cross-section. It is shown herein that this method assumes that a unique plate buckling coefficient, or *k* value, exists for each element of a section, and that the web-flange interaction is thus at a fixed amount. In reality, as demonstrated herein with finite strip analysis, the local plate buckling coefficients vary widely for a given section and loading. However, the variation in *k* may be expressed as a function of the member geometry and loading and simple relations are provided for such *k*, which include web-flange interaction. The developed expressions provide a potential first step towards rationalizing the AISC Specification approach to local buckling limit states across the different sections.

ACKNOWLEDGEMENTS

The authors of this paper gratefully acknowledge the financial support of AISC, and the AISC Faculty Fellowship program in this research. In addition, a portion of this work was initiated in collaboration with Don White during the development of the 2005 AISC Specification, many thanks to Don for his contributions in this regard. Of course, any views or opinions expressed in this paper are those of the authors alone.

REFERENCES

[1] AISC (2005), *"Specification for Structural Steel Buildings"*, American Institute of Steel Construction, Chicago, IL. ANSI/ASIC 360-05, 2005.

[2] AISI (2007), *"North American Specification for the Design of Cold-Formed Steel Structures"*, American Iron and Steel Institute, Washington, D.C., AISI-S100, 2007.

[3] Bijlaard, P.P., Fisher, G.P., *" Column Strength of H-Sections and Square Tubes in Post-Buckling Range of Component Plates"*, NACA, TN 2994, August, 1953.

[4] Bulson, P.S., *"The Stability of Flat Plates"*, Chatto and Windus, London, 1970.

[5] Galambos, T., *"Guide to Stability Design Criteria for Metal Structures"*, 5th edition, Wiley, New York, NY, 1998, 815-822.

[6] Hancock, G. J., *"Local, Distortional, and Lateral Buckling of I-Beams"*, ASCE J Struct Div, v 104, n 11, Nov, 1978, p 1787-1798.

[7] Salmon, C.G., Johnson, J.S., *"Steel structures: design and behavior: emphasizing load and resistance factor design"*. 5th edition, Pearson, Prentice Hall, Upper Saddle River, New Jersey, 2009.

[8] Schafer, B.W., Ádány, S., *"Buckling analysis of cold-formed steel members using CUFSM: conventional and constrained finite strip methods"* Proceedings of the Eighteenth International Specialty Conference on Cold-Formed Steel Structures, Orlando, FL., 2006, 39-54.

[9] Von Karman, T., Sechler, E.F., Donell, L.H., *"Strength of Thin Plates in Compression"*, American Society of Mechanical Engineers -- Transactions -- Applied Mechanics, v 54, n 2, Jan 30, 1932, p 53-56.

[10] White, D.W., *"Unified Flexural Resistance Equations for Stability Design of Steel I-Section Members: Overview"*, Journal of Structural Engineering, v 134, n 9, 2008, p 1405-1424